NUMERICAL STUDIES ON METAL HYDRIDE COMPOSITE SOFT ACTUATORS

G. Mohan, Bharath Ram, Gokul Das
Centre for Computational Research in Clean Energy Technologies, Sree Chitra Thirunal College of Engineering, Thiruvananthapuram, Kerala, India.

Abstract
Self-actuating materials adapt their structure and functionality in response to external stimuli, presenting fascinating properties and diverse applications. Metal hydrides have garnered extensive attention as promising materials for hydrogen storage. Given the notable swelling observed during hydrogenation, composites incorporating flexible materials hold promise as candidates for soft actuators. In this study, COMSOL Multiphysics™ commercial code is employed to conduct a numerical simulation of the performance of soft sheet composite actuator utilizing $LaNi_5$ within silicone rubber matrix.

Keywords: Actuator, Metal Hydride, $LaNi_5$, Hydrogen, Simulation.

Introduction
In recent years, there has been a surge of interest in bio-mimicking self actuation materials and technologies, due to their interesting properties and potential applications . Additionally, many of these materials are environmentally benign. These materials, often classified as intelligent or smart materials, exhibit reversible alterations in functionality and structure in response to external stimuli. This unique characteristic enables them to serve as both sensors and actuators within a single entity [1].

Historically, metal hydrides have been recognized for their favorable charge-discharge attributes, including high volumetric storage capacity, rapid sorption kinetics, extended cyclic lifespan, and enhanced safety, making them popular as hydrogen storage media. Nevertheless, their potential as storage materials has been constrained by their limited gravimetric storage capacity. Notably, materials like $LaNi_5$ undergo reversible volume changes during hydrogenation, with lattice expansion reaching nearly 25%. This phenomenon arises from the occupation of interstitial sites within the metallic matrix by hydrogen atoms.

While numerous studies have explored the thermal performance of metal hydride-based solid-state devices [2], encompassing analyses of storage beds, few have delved into the mechanical actuation potential derived from the expansion and shrinkage of metal hydrides. Mellouli et al. [3] conducted a seminal experimental study, directly observing the volumetric changes of a $LaNi_5$ granular bed in a transparent metal hydride reactor. Their findings underscore a significant shift in the specific volume of the granular bed throughout the charging-discharging process. Yumiko et al. [4] delved into the swelling and shrinkage behaviors of $LaNi_5$-based alloys, revealing that these phenomena are contingent on the width of the plateau region. Furthermore, Nachev et al. [5] employed dilatometry to measure the progressive swelling of ball-milled MgH_2 compacted disks upon cyclic hydrogenation, demonstrating a cumulative displacement that stabilizes after 30 cycles. Briki et al. [6] conducted experimental studies on the expansion of $LaNi_5$ compacted powder during hydrogen charge-discharge cycles, revealing that as long as hydrogenation remains fully reversible, expansion can be likewise reversible. However, this process is dependent on heat transfer as a major rate-limiting factor.

Kagawa et al. [7] studied the response characteristics of copper-encapsulated metal hydride-based bending actuators, revealing the enhanced performance achieved with the addition of copper. Similarly, Nakai et al. [8] investigated the bending and rotation of a palladium-coated metal hydride-based actuator, observing improved displacement with minimal copper thickness. These studies emphasize the pivotal role of heat transfer in governing the response behavior of hydride-based actuation devices. Studies have also been carried out on hydrogen gas pressure driven actuators in flexible systems like artificial muscles [9-11]. Y. Nishi et al. [12] studied the performance of a soft bimorph actuator comprising of two rubber sheets, one dispersed with $LaNi_3Co_2$ powder. The strains induced upon hydrogenation was found to be significant.

The metal hydride based soft composites can undergo interesting deformation upon hydrogenation. This study undertakes numerical simulations of the deformation characteristics of $LaNi_5$-Silicone rubber composite upon hydrogenation. These simulations are conducted using the COMSOL Multiphysics™ commercial code.

Physical Model

Figure 1 shows the schematic of metal hydride based composite actuator with $LaNi_5$ as the hydrogenation alloy. The actuating element is an overlapping layered composite in which $LaNi_5$ powder embedded with Silicone Rubber in alternate layers. The actuator is divided into six sections where the layers of metal hydride and rubber are placed alternatively, one layer on top and the other at the bottom, adjacent to each other. Hydrogen is supplied through the arteries given inside the composite. The actuating element is encapsulated in the given housing through which coolant is circulated at the given temperature.

Once hydrogen is inducted to the actuator element at the given pressure, the reaction commences and gas is absorbed by the alloy. This leads to swelling of the alloy particles which leads to the distortion of the actuating member. However, the peculiar arrangement causes the deformation of each section to be opposite, with respect to the adjacent section. This causes the actuator to develop a wavy deformation.

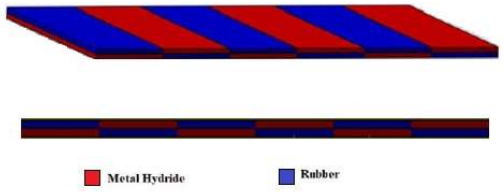

Fig. 1 Schematic of metal hydride based composite actuator

Governing Equations

Mass balance of metal

Mass balance of hydride is given by the following equation.

$$(1-\phi)\frac{\partial \rho_s}{\partial t} = \dot{m} \qquad (1)$$

$\dot{m}$ stands for the rate of hydrogen absorbed.

Sorption kinetics

For hydriding/dehydriding, rate of hydrogen entering/leaving the alloy is given by the following eqns. [13].

$$\dot{m}_a = C_a \exp\left(-\frac{E_a}{RT}\right) \ln\left(\frac{P}{P_{eq}}\right)(\rho_{sat} - \rho_s) \qquad (2)$$

$$\dot{m}_d = C_d \exp\left(-\frac{E_{ad}}{RT}\right) \left(\frac{P-P_{eq}}{P_{eq}}\right)(\rho_s - \rho_a) \qquad (3)$$

where C_a and C_d are the rate constants for hydrogen absorption and desorption respectively.

Equilibrium pressure (P_{eq}) is determined using van't Hoff equation as given below

$$\ln P_{eq} = A - \frac{B}{T} \qquad (4)$$

Energy balance

Heat conduction in the hydriding alloy is given by the general heat diffusion equation as given below.

$$(\rho C_p)_e \frac{\partial T}{\partial t} = \lambda_e \frac{\partial}{\partial x}\left(\frac{\partial T}{\partial x}\right) + \lambda_e \frac{\partial}{\partial y}\left(\frac{\partial T}{\partial y}\right) + \lambda_e \frac{\partial}{\partial z}\left(\frac{\partial T}{\partial z}\right) + \dot{m}\Delta H^0 \qquad (5)$$

Effective heat capacity of the porous composite can be determined as follows.

$$(\rho C_p)_e = \phi \rho_H C_{pH} + (1-\phi)\rho_s C_{ps} \qquad (6)$$

The effective thermal conductivity of the composite can be determined by the following equation.

$$k_e = \phi k_H + (1-\phi)k_s \qquad (7)$$

Stress-strain equations

The wall stresses on the actuator element can be due to combined volumetric and thermal expansion of hydride and is found to be linear with temperature [14]. This is represented by the following eqn. [15]

$$\alpha_e = \alpha\left[1 + \alpha\Delta T + \frac{0.167}{3\alpha\Delta T}\left(1 - \left[\frac{C_{sat}-C}{C_{sat}-C_0}\right]\right)\right] \qquad (8)$$

where 'α 'designates the coefficient of thermal expansion.

The effective elastic modulus of the porous hydride bed can be computed as given below [16].

$$Y_e = Y_0\left(1 - \frac{\phi}{\phi_{cr}}\right)^p \qquad (9)$$

where Y_0 is the elastic modulus of non-porous material. ϕ and ϕ_{cr} are the actual and critical porosities respectively. 'p' is a material specific exponent.

The total stress developed is due to the volumetric expansion of hydride, thermal expansion and gas pressure. This can be computed by the equilibrium equations, strain-displacement relations and constitutive equations. Ramberg-Osgood model [17] represents the non linear characteristic of the material in the plastic regime.

$$\epsilon = \frac{\sigma}{Y} + 0.002\left(\frac{\sigma}{\sigma_{0.2}}\right)^n \qquad (10)$$

where

$$n = \frac{\ln 20}{\ln\left(\frac{\sigma_{0.2}}{\sigma_{0.01}}\right)} \qquad (11)$$

$\sigma_{0.2}$ is the 0.2% proof stress and *n* denotes the strain hardening exponent.

Initial and boundary conditions

The initial conditions of hydride:

$$\rho_s = \rho_{s0}; \quad p = p_0; \quad T = T_0 \ \ at\ t = 0 \quad (12)$$

The convective heat transfer at the outside surface of actuator element is given below.

$$-k_e \nabla T = U(T_f - T) \quad (13)$$

For the inner artery supplying the gas, boundary conditions are applied as follows.

$$P = P_H; \quad \frac{\partial T}{\partial r} = 0 \quad (14)$$

Simulation Methodology

Numerical simulations of actuator deformation during hydrogen absorption/desorption are performed with COMSOL Multiphysics® commercial software. Heat transfer, chemical species and structural mechanics modules with suitable multi-physics coupling were used to implement the given mathematical model. Initial and boundary conditions are applied as per the given formulation. Meshing is done with tetrahedral elements of given element size. The economic size of the mesh is determined by grid independence study. Time dependent iterative solver is used for solution of the problem. The results are plotted using the post processing capabilities of the software.

Results and Discussion

$LaNi_5$ is chosen as the hydriding alloy due to its high sorption rates, good hydrogen storage capacity, low plateau slope and low hysteresis. Hydrogen sorption is limited by heat transfer in most applications.

Table 1: *Thermophysical properties of $LaNi_5$* [18] *and silicone rubber used in simulation*

Properties	$LaNi_5$	Silicone Rubber
Density (kg m^{-3})	8200	2300
Specific heat($Jkg^{-1}K^{-1}$)	419	1300
Thermal conductivity ($Wm^{-1}K^{-1}$)	30	2.5
Activation energy (abs),E_a($J\ mol^{-1}$)	21170	
Activation energy (des),E_d($J\ mol^{-1}$)	16420	
Constants in reaction kinetics equation C_a, s^{-1} A B	 59.187 12.99 3704.59	
Modulus of elasticity, E (GPa)	140	0.05
Poisson's ratio, ν	0.31	0.49
Coefficient of thermal expansion, α (K^{-1})	1.23e-5	3e-4

The physical properties of $LaNi_5$ and silicon rubber are given in Table 1. Simulations are performed for the given device during absorption and desorption.

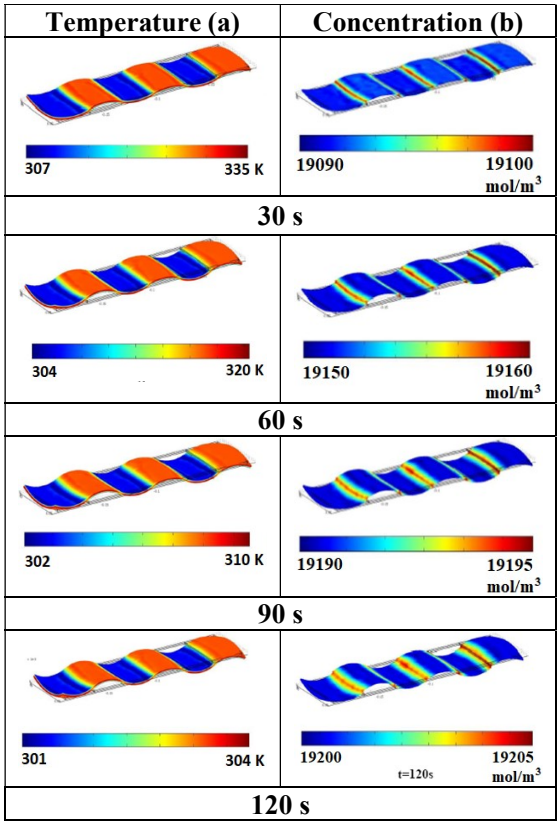

Fig. 2: *Spatial variation of temperature and concentration of actuator element at different time intervals during hydrogenation*

Figure 2a shows the spatial variation of temperature at different time intervals during hydrogenation. Temperature at the regions close to the interfaces are lower due to higher rate of heat conduction. Temperature increases rapidly during the initial stages due to high rate of hydrogen absorption. However this decreases later due to lower hydrogenation rates as most regions are saturated and reaction stops.

Figure 2b shows the corresponding variation of hydrogen concentration at different time intervals. Concentration near the interfaces is higher compared to the rest of the device. This is attributed to the correspondingly lower temperature in those regions. Low temperature causes higher differential between gas pressure and equilibrium pressure leading to higher rates of reaction. Concentration also increases with time till saturation. This leads to higher deformation of the actuator element.

Figure 3a shows spatial variation of temperature at different time intervals during desorption. Higher rate of heat conduction from silicon rubber to metal

hydride is observed at the interfaces. This leads to higher temperature in those regions which leads to lower hydride concentration in those regions as shown in Fig. 3b. As time elapses, hydride concentration decreases due to desorption which causes the actuator element to retain its original shape.

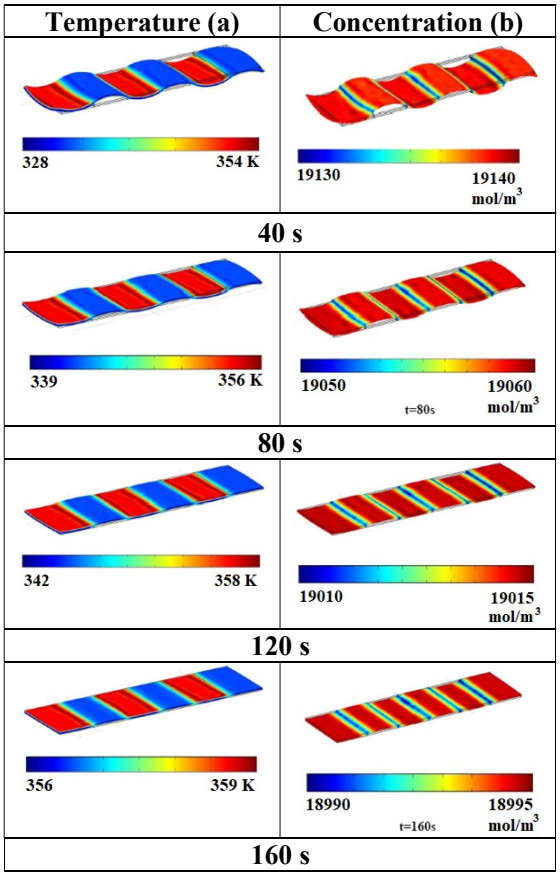

Fig. 3: *Spatial variation of temperature and concentration of actuator element at different time intervals during dehydrogenation*

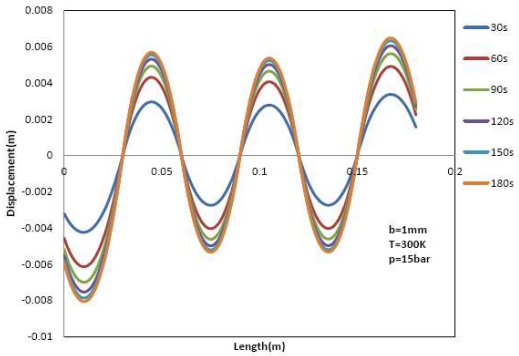

Fig. 4: *Variation of actuator displacement along its length during hydrogenation*

Figure 4 shows the variation of actuator displacement along its length. The sheet exhibit a wavy deformation due to the intricate placement of the metal hydride. While the sections where metal hydride is provided as top layer exhibit a convex bend, the sections with bottom layer of the alloy deforms in the opposite direction. This is due to the differential expansion of the two materials. Upon hydrogenation, as time elapses, the differential expansion increses due to higher volumetric swelling. Higher deformation is also observed at the free ends.

Conclusions

Numerical simulations are performed for the hydrogenation and dehydrogenation of metal hydride based composite actuator. Based n the results, it is found that the distinctive arrangement of the storage alloy within the silicone rubber matrix induces a characteristic wavy deformation. Charge-discharge cycles can generate pulsations within the device which can be promising for numerous applications. As heat transfer is the major controlling factor affecting hydrogenation in metal hydrides, the response characteristics of these devices can be improved by heat transfer enhancement.

Acknowledgments

This study is supported by All India Council for Technical Education (AICTE) under RPS scheme.

References

[1] Y. Liu, Y. Zhong and C. Wang, Recent advances in self-actuation and self sensing materials: State of the art and future perspectives. *Talanta* 2020;212, pp.120808.

[2] S. Srinivasa Murthy, Heat and mass transfer in solid state hydrogen storage: A review. *J. Heat Transfer* 2012; 134, pp. 1-11.

[3] S. Mellouli, F. Askri, H. Dhaou, A. Jemni and S. Ben Nasrallah, Study of the thermal behavior of a deformable metal-hydridebed. *Int J Hydrogen Energy* 2016;41, pp. 1711-1724.

[4] N. Yumiko, S. Kouichi, F. Shin, N. Koji, O. Keisuke and U. Itsuki, Lattice expanding behaviour and degradation of LaNi5-based alloys. *Journal of Alloy Comp* 1998;267, pp. 205-210.

[5] S. Nachev, P. De Rango, B. Delhomme, D. Plante, B. Zawilski, F. Longa, Ph. Marty, S. Miraglia and D. Fruchart, In situ dilatometry measurements of MgH_2 compacted disks. *Journal of Alloy Comp* 2013;580, pp. 183-186.

[6] C. Briki, P. Rango, S. Belkhiria, M.H. Dhaou and A. Jemni, Measurements of expansion of $LaNi_5$ compacted powder during hydrogen absorption/desorption cycles and their influences on the reactor wall. *International Journal of Hydrogen Energy* 2019;44, pp. 13647-13654.

[7] A. Kagawa, K. Taniguchi and M. Yamamoto Design of miniaturization of bending actuators

utilizing hydrogen storage alloy. *Journal of Alloy and Compounds* 2013;563, pp. 203-206.

[8] A. Nakai, M. Mizumoto and A. Kwaga, Bending and rotation movement control of a novel actuator using hydrogen storage alloys. *Advanced Material Research* 2011;156-157, pp. 1170-1175.

[9] G. M. Lloyd and K. J. Kim, Smart hydrogen/ metal hydride actuator, *International Journal of Hydrogen Energy* 2007;*32*, pp. 247-255.

[10] K. Jung and K. J. Kim, A Thermo kinetically Driven Metal-Hydride Actuator, *Proceedings of SPIE Sensors and Smart Structures Technologies for Civil, Mechanical and Aerospace Systems* 2008, 6932.

[11] M. Hosono, S. Ino, M. Sato, K. Yamashita and T. Izumi, A System Utilizing Metal Hydride Actuators to Achieve Passive Motion of Toe Joints for Prevention of Pressure Ulcers: A Pilot Study, *Rehabilitation Research and Practice*, (2012)

[12] Y. Nishi, H. Uchida, H. Yabe, B. Kim and T. Ogasawara, Giant Bending Motion of a Soft Actuator Controlled by Hydrogen Gas Pressure, *Journal of Intelligent Material Systems and Structures;* 2006; 17(8), pp. 709-711.

[13] F. Askri, A. Jemni and S. B. Nasrallah, Study of two dimensional and dynamic heat mass transfer in a metal hydrogen reactor. International Journal of Hydrogen Energy 2003; 28, pp. 537-57.

[14] J. M. Joubert, R. C. Cerny, M. Latroche, A. Parcheron-Guegan and K. Yvon, Compressibility and Thermal expansion of LaNi5 and substitutional derivatives. Intermetallics 2005; 13, pp. 227- 31.

[15] D. Lekshmi and G. Mohan, Numerical simulation of the parametric influence on the wall strain distribution of vertically placed metal hydride based hydrogen storage container. International Journal of Hydrogen Energy 2015; 40, pp. 5689-5700.

[16] K. K. Phani and S. K. Niyogi, Youngs Modulus of Porous Brittle Solids. Journal of Material Science 1987; 22, pp. 257-63.

[17] W. R. Osgood and W. Ramberg, Description of stress strain curves by three parameters. NACA Technical Note 902, Washington DC: National Bureau of Standards; 1943.

[18] Hymarc. *Hydrogen Storage Mat. Database - Data and Resources.* https://datahub.hymarc.org/dataset/hydrogen-storage-materials-db